Adaptive Receiver for Visible Light Communication System

Aubida A. Al-Hameed[1], Ahmed Taha Hussein[1], Mohammed T. Alresheedi[2] and Jaafar M. H. Elmirghani[1]
[1]School of Electronic and Electrical Engineering, University of Leeds, Leeds, LS2 9JT, UK
[2]Department of Electrical Engineering, King Saud University, Riyadh, Saudi Arabia
E-mail: {elaawj@leeds.ac.uk, ml12ath@leeds.ac.uk, malresheedi@ksu.edu.sa, j.m.h.elmirghani@leeds.ac.uk}

ABSTRACT
The future of visible light communication (VLC) systems relies on achieving moderate to high data rates and the ability to design a low complexity system, as these will play a major role in the next generation communication networks. In this paper, we propose, design, and evaluate the use of an adaptive receiver to mitigate the inter-symbol interference (ISI) and improve the overall VLC system performance while using a single element wide field of view (FOV) photodetector. In addition, we optimise the adaptive receiver by employing a different number of buffers to find the optimum configurations in terms of reducing the complexity and achieving the best performance. The proposed adaptive receiver is able to provide data rates of 1 Gbps with a BER of 10^{-5} for OOK modulation in the worst case scenario.

1. INTRODUCTION

Visible light communication (VLC) is a type of optical wireless communication (OWC) system that uses light as a carrier to modulate the information signal in the visible spectrum (380nm to 780 nm) [1].The interest in VLC has rapidly increased due to the possibility of integrating the high-speed communication network with an illumination system by using light emitting diodes (LED) as a light source and a transmitter to encode the data signal with the illumination light; thus, VLC is a cost-effective and energy efficient system [1], [2]. VLC systems have many advantages compared to radio frequency (RF) systems, such as there is no interference with radio systems, a more secure connection because light cannot penetrate walls, and a free unlicensed broad spectrum [2], [3]. VLC is preferred over infrared (IR) communication systems due to eye safety, in addition to the illumination function of visible light. LEDs also have many beneficial properties, such as low power consumption, low cost, and long lifetime. Recently, the novel architecture of a laser diode (RGB-LD) with combiner and diffuser has been proposed as a new VLC transmitter [4]. For the single carrier modulation of a VLC system, the delay spread of the channel at a high data rate can become larger than the transmitted symbol duration, which causes a high inter-symbol interference (ISI) that leads to a degradation in the performance of the VLC system in terms of the bit error rate. Many techniques have been proposed to minimize the ISI effect for single element photodetector (PD) receivers. Block decision-feedback equalization (BDFE) and parallel decision-feedback decoding (PDFD) for the wireless optical channel were first deployed to reduce the effect of the ISI in single carrier wireless IR systems [5]. Block-based pulse amplitude modulation (PAM) with DFE has been presented for VLC with improvements up to a 60 MHz bandwidth [6]. An adaptive equalizer has been introduced to overcome ISI, and a DFE equalizer can be used for data rates over 700 Mbps [7]. A spread spectrum technique has also been proposed to reduce the ISI [8].

Multi-carrier modulation, such as orthogonal frequency division multiplexing (OFDM), has been used by [9] to combat the ISI effect. The VLC system can use a DC-biased optical DCO-OFDM and blue LED. This system has demonstrated a data rate of up to 513 Mbps [10]. An 800 Mbps data rate was achieved in a VLC system by using a DCO-OFDM and RGB-LED [11]. A RGB-LED and adaptive DCO-OFDM VLC system was introduced with up to a 3.4 Gbps data rate [12].

Previous work has shown that a wide FOV receiver can only support low data rates (up to 50 Mbps) [3], [13]. A single photodetector receiver using rake reception with adaptive equalization has been proposed in [14], and up to 200 Mbps has been achieved with a bit error rate (BER) of 10^{-5}. Expensive and highly complex receivers, such as an angle diversity receiver (ADR) and an imaging receiver, have been proposed to mitigate ISI and improve the performance of the OW system to provide multi-gigabit data rates [15], [16]. A delay adaptation technique with imaging receiver has been proposed to combat ISI and provide high data rates of up to 10 Gbps [4]. VLC systems have the potential to play a major part in the next generation of communication networks and future smart homes. There is significant on-going work to achieve high data rate VLC systems [17]; however, an increase in the system complexity and receiver cost is incurred.

In this paper, a novel adaptive receiver is proposed with optimum configurations for VLC systems to provide high data rates (1 Gbps) and also to reduce the size and cost of multiple non-imaging angle diversity receivers and imaging receivers. The reminder of this paper is divided into sections as follows: Section 2 introduces the simulation environment and room setup. Section 3 presents the VLC systems' configurations. Simulation results and discussions are presented in Section 4. Finally, conclusions are drawn in Section 5.

2. SIMULATION ENVIRONMENT AND ROOM SETUP

To evaluate the performance of the proposed receiver for an indoor VLC system, a simulation was performed in an empty room with the dimensions of 4 m × 8 m × 3 m (width × length × height), as shown in Fig. 1. Eight light units were used to satisfy ISO and European standards (i.e., 300 lx) [4]. The light units were placed at a height of 3m above the floor, each unit had nine RGB-laser diodes (LDs), and the transmitted power from each LD was 2 W with a semi-angle at half power beam width of 70^{o} [13]. The simulation was based on a ray-tracing algorithm. Previous experimental measurements of plaster walls have shown that the reflected light rays were similar to the Lambertian model, thereby the light reflections from the floor, walls, and ceiling were modelled as a Lambertian pattern with reflection coefficients of 0.3 for the floor and 0.8 for the walls and ceiling; also, reflections from doors and windows were assumed to be the same as the walls. The room was divided into a number of reflection elements that had square areas (5 cm × 5 cm for the first order reflection and 20 cm × 20 cm for the second order reflection) and the same reflection coefficient, and each reflection element was considered as a secondary transmitter that transmited an attenuated copy of the received signal from its centre. The height of the communication floor (CF), where the transmitters and receivers for the user's equipment were placed, was 1 m. The simulation and calculations in this paper were carried out using the MATLAB program. Our simulation tool was similar to one developed by Barry et al. [18]. In our evaluation, the channel response and SNR were determined in a similar way as that used in [4], [19].

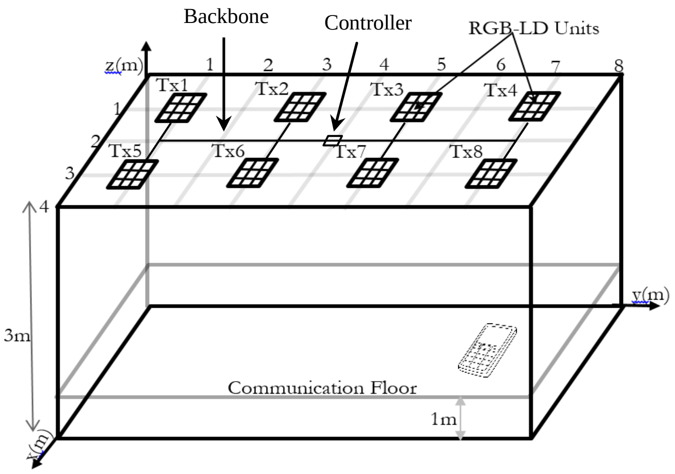

Figure 1. VLC system room.

3. VLC SYSTEM CONFIGURATION

In this section, two VLC receivers are presented, analysed, and compared to identify the most appropriate system for use in an indoor environment with a mobile user.

3.1 Traditional Wide-FOV Receiver (TWFR)

A single element receiver with wide FOV (90^{o}) and photo sensitive area of 4 mm^{2} was used. A traditional single optical receiver with wide FOV is the most basic receiver configuration that has been widely investigated in previous research [3], and it is considered here to compare it with our new proposed adaptive VLC receiver. A receiver with a wide FOV gathers more optical power than a narrow FOV receiver, because a wide FOV receiver collects not only the primary signal (line of sight component), but also signals that have one or more reflections, thus increasing the received signal power. On the other hand, multipath dispersion can cause signal spread.

3.2 Adaptive Wide-FOV Receiver (AWFR)

The newly proposed adaptive receiver has the same characteristics as a traditional wide FOV (i.e., 90^{o} and 4 mm^{2}). However, three new stages were added to the traditional receiver to process the received optical signal to enable the system to achieve data rates higher than 50 Mbps.

The proposed adaptive receiver uses a simple amplitude equalization technique for the line of sight (LOS) components of the received signal power. The received signal is sampled at different time points and then the captured signals are delayed. Fig. 2 shows a block diagram of the proposed adaptive receiver. The adaptive receiver consists of four stages: the first stage is a single wide-FOV photodetector that collects the LOS and reflected light rays (up to second reflections) that were emitted from different active transmitters. The second stage is a switching mechanism working as a sampler to sample the received signal. Sampling time depends on the estimated channel delay profile (channel delay profile is estimated by controller and sent to the receiver over control channel). The third stage includes multiple holding buffers, and each buffer holds a sampled signal for a certain time duration according to the channel delay profile. Each buffer can be represented by a time shifted matched filter. The number of buffers depends on the channel delay profile as well. After holding the sampled signals, an equal gain combiner (EGC) is used to maximise the SNR. Finally, a hard decision circuit is used to recover the received data.

3.3 Power received analysis of TWFR and AWFR

The total received power P_R for the user on the CF consist of the received LOS power P_{LOS} and the power due reflections $P_{reflections}$. The total received power is given as:

$$P_R = P_{LOS} + P_{reflections} \tag{1}$$

In this paper, we considered the LOS as well as the first and second order reflections. In the mathematical analysis below we focused only on the LOS component to simplify the explanation of the equations. The received LOS power ($P\mathrm{TWFR}_{LOS}$) of traditional wide-FOV receiver written as:

$$P\mathrm{TWFR}_{LOS}(t) = \sum_{i=1}^{k} \alpha_i P_{txi}(T + d_i) \tag{2}$$

where T is the symbol duration time, k is the number of active transmitters, d is the time delay from each transmitter, and α is the attenuation factor due to the signal propagation, where ($\alpha_1 < \alpha_2 ... << \alpha_n$). A severe ISI occurs when the symbol time T is much smaller than the maximum delay ($T << d_{Max}$). The received LOS power ($PAWFR_{LOS}$) of the proposed adaptive receiver AWFR written as:

$$PAWFR_{LOS}(t) = \sum_{n=1}^{N} \left(\left(\sum_{i=1}^{k} \alpha_i P_{txi}(T + d_i) \right) G\, u(Ts_n - Th_n) \right) \tag{3}$$

where N is the number of buffers, G is the weight factor of the equal gain combiner, Ts is the sampling time, Th is the holding time and $u(t)$ is the unit step function.

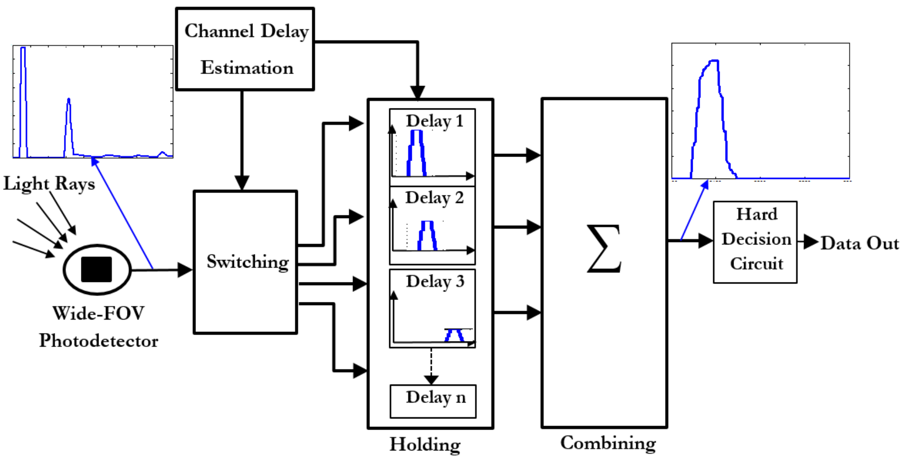

Figure 2. Block diagram of adaptive receiver.

4. SIMULATION RESULTS AND DISCUSSION

In this section, we assess the performance of the proposed adaptive receiver using a simple wide-FOV photodetector for the VLC system in an empty room in the presence of multipath propagation and mobility. A comparison between the TWFR and new AWFR was performed and is presented. The increased number of buffers in the adaptive receiver is also discussed with regards to the optimum configuration as well. The proposed systems were examined for a single user with mobility in fourteen different locations along the x-axis and y-axis. The results are presented in terms of impulse response and SNR. The results for x=3 were equal to the results for x=1 due to the symmetry of the room.

4.1 Received Pulse Response

The received pulse responses of the VLC system using the TWFR and AWFR for different locations on the CF (1m, 1m, 1m), (1m, 4m, 1m), (2m, 1m, 1m), and (2m, 4m, 1m) are presented in Fig. 3. Each pulse response includes LOS as well as first order and second order reflection components. The signal spread of the received pulse response depends on the location of the receiver on the CF. It should be noted that the received pulse response of the receiver at the room centre (2m, 4m, 1m) consists of two LOS ray components. The first LOS component was collected from the light emitted by the transmitters T_{X2}, T_{X3}, T_{X6}, and T_{X7} (see Fig. 1) due to the same distance separating the transmitters and receiver. The second LOS component was collected from the transmitters T_{X1}, T_{X4}, T_{x5}, and T_{x8}. It can be clearly seen that the AWFR's pulse response (see Fig. 3) is better than that of the TWFR in terms of signal spread. The pulse response of the TWFR contains many peaks that correspond to different direct LOS components coming from different LD light units.

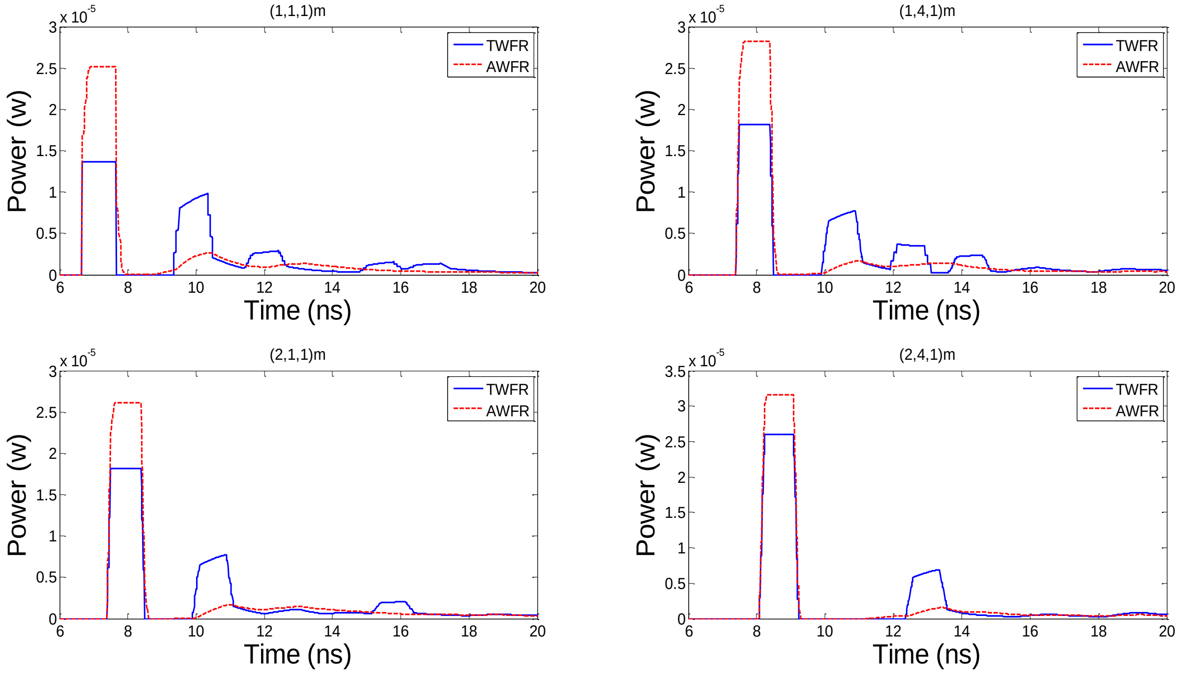

Figure 3. Pulse responses of TWFR and AWFR receivers at different location on CF.

4.2 SNR Analysis of TWFR and AWFR

Fig. 4 shows the SNR of the TWFR and AWFR at a bit rate of 1 Gbps, and a wide band CMOS optical receiver was considered for the SNR calculations [20]. The results show a significant improvement in the SNR under the AWFR when compared with the TWFR. For the worst case scenario, the AWFR achieved a 10 dB SNR gain over the TWFR when the receiver moved along x=1m, and about a 6 dB SNR gain along x=2m. As shown in the results, the minimum SNR for the AWFR was about 7.5 dB at the room corner (x=1 and y=1). For OOK modulation an SNR of 7.5 dB can provide a BER of 10^{-5}. A low-complexity forward error correction (FEC) technique can be used to improve the BER (to further reduce the BER from 10^{-5} to 10^{-9}) for optical systems operated at a few gigabits [21]. From the results obtained in this section it can be clearly seen that TWFR does not support high data rates with an acceptable BER.

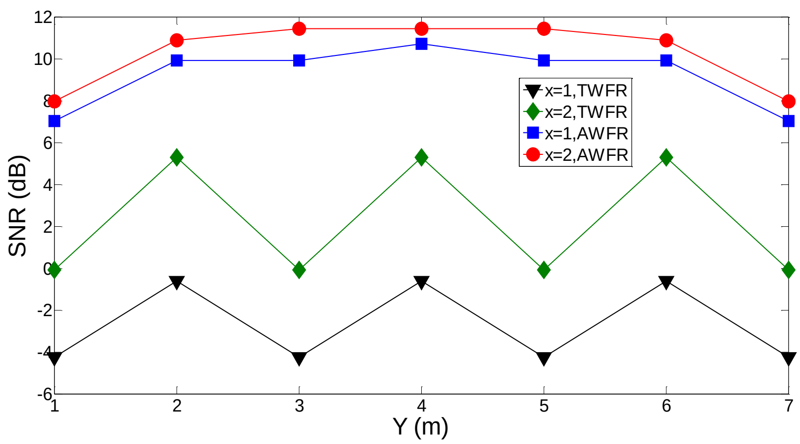

Figure 4. SNR of TWFR and AWFR systems at x=1m and x=2m.

4.3 SNR Analysis of Multiple Buffers Configuration in AWFR

Different amounts of buffers were examined to find the optimum configurations of the adaptive receiver in terms of reducing the complexity and providing good performance (seven buffers is considered as ideal case). Fig. 5 presents the SNRs of the user moving along the y-axis at x=1m and x=2m, respectively. It can be clearly seen that the number of required buffers depends on the receiver location on the CF, which is due to the characteristics of the pulse response for the VLC indoor channel as shown in Fig. 3. The results show that five buffers are the optimum configuration for the mobile adaptive receiver when it moves at x=2m along the y-axis. However, there is a performance degradation in the AWFR in terms of the SNR for four locations at x=1m on the CF as shown in Fig. 5a.

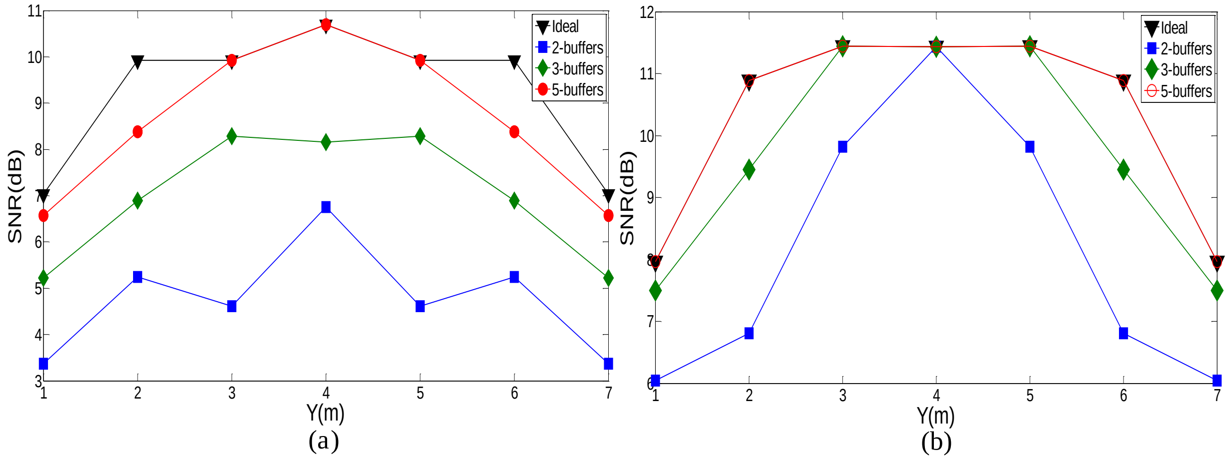

Figure 5. (a) SNR of multiple buffers configuration for AWFR at x=1m. (b) SNR of multiple configuration buffers for AWFR at x=2m.

In Fig. 6, the SNR penalty was calculated for the AWFR with movement along the y-axis at x=1m and x=2m. The results show that the SNR penalty occurred due to the mobility of the AWFR on the CF. The five buffer configurations for the AWFR can provide a similar performance to the ideal case when seven buffers were used, and it is a trade-off configuration between increasing the complexity and reducing the system performance. However, the maximum SNR penalty was about 1.5dB for the worst case locations of x=1m, y=2m and x=1m, y=5m. To reduce the complexity of the calculations at the receiver side, a handshaking signal is exchanged between the controller and the receiver before starting to send data. The receiver estimates the delay profile of the channel during the initialisation setup by sending a pilot signal. The feedback signal is sent through an uplink IR-OW connection to the controller. The controller is responsible for identifying a number of buffers for the receiver in each location on the CF according to the SNR penalty and channel quality (BER).

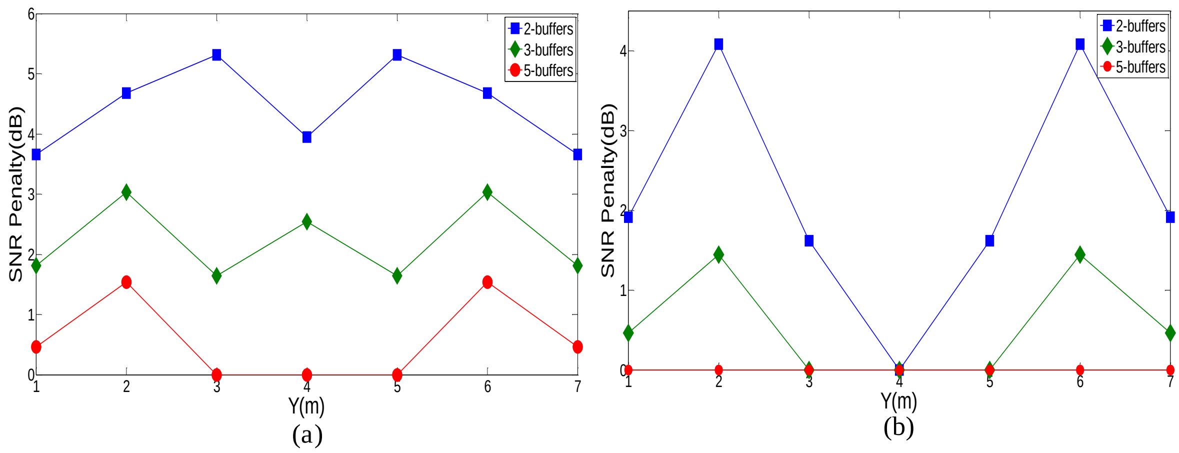

Figure 6. (a) SNR penalty of multiple buffers configuration for AWFR at x=1m. (b) SNR penalty of multiple buffers configuration for AWFR at x=2m.

5. CONCLUSIONS

We proposed, designed, and investigated a novel adaptive receiver that uses a single wide-FOV photodetector. The adaptive receiver achieved 1 Gbps and a BER of 10^{-5} at the least successful point in an empty room with the simple modulation format (OOK). Our proposed AWFR for a VLC system has the ability to increase the SNR from 0.2 dB to 7.5dB in the room's corners. The margin of SNR penalty for a five buffers configuration was about 1.5dB, which compared well to the ideal configuration of seven buffers at two locations on the CF.

REFERENCES

[1] H. Burchardt, N. Serafimovski, D. Tsonev, S. Videv, and H. Haas, "VLC: Beyond point-to-point communication," Communications Magazine, IEEE, vol. 52, no. 7, pp. 98-105, 2014.

[2] H. Elgala, R. Mesleh, and H. Haas, "Indoor optical wireless communication: potential and state-of-the-art," Communications Magazine, IEEE, vol. 49, no. 9, pp. 56-62, 2011.

[3] T. Komine and M. Nakagawa, "Fundamental analysis for visible-light communication system using LED lights," Consumer Electronics, IEEE Transactions on, vol. 50, no.1, pp. 100-107, 2004.

[4] A. T. Hussein and J. M. Elmirghani, "Mobile multi-gigabit visible light communication system in realistic indoor environment," Journal of Lightwave Technology, vol. 33, no. 15, pp. 3293-3307, 2015.

[5] D. C. Lee and J. M. Kahn, "Coding and equalization for PPM on wireless infrared channels," in Global Telecommunications Conference, 1998. GLOBECOM 1998. The Bridge to Global Integration. IEEE, 1998, pp. 201-206.

[6] L. Grobe and K.-D. Langer, "Block-based PAM with frequency domain equalization in visible light communications," in Globecom Workshops (GC Wkshps), 2013 IEEE, 2013, pp. 1070-1075.

[7] T. Komine, J. H. Lee, S. Haruyama, and M. Nakagawa, "Adaptive equalization system for visible light wireless communication utilizing multiple white LED lighting equipment," Wireless Communications, IEEE Transactions on, vol. 8, no. 6, pp. 2892-2900, 2009.

[8] K. Wong and T. O'Farrell, "Spread spectrum techniques for indoor wireless IR communications," Wireless Communications, IEEE, vol. 10, no. 2, pp. 54-63, 2003.

[9] N. Saha, R. K. Mondal, N. T. Le, and Y. M. Jang, "Mitigation of interference using OFDM in visible light communication," in ICT Convergence (ICTC), 2012 International Conference on, 2012, pp. 159-162.

[10] J. Vučić, C. Kottke, S. Nerreter, K.-D. Langer, and J. W. Walewski, "513 Mbit/s visible light communications link based on DMT-modulation of a white LED," Journal of Lightwave Technology, vol. 28, no. 24, pp. 3512-3518, 2010.

[11] J. Vucic, C. Kottke, K. Habel, and K.-D. Langer, "803 Mbit/s visible light WDM link based on DMT modulation of a single RGB LED luminary," in Optical Fiber Communication Conference, 2011, p. OWB6.

[12] G. Cossu, A. Khalid, P. Choudhury, R. Corsini, and E. Ciaramella, "3.4 Gbit/s visible optical wireless transmission based on RGB LED," Optics express, vol. 20, no. 12, pp. B501-B506, 2012.

[13] A. T. Hussein and J. M. Elmirghani, "High-speed indoor visible light communication system employing laser diodes and angle diversity receivers," in Transparent Optical Networks (ICTON), 2015 17th International Conference on, 2015, pp. 1-6.

[14] M. Biagi, T. Borogovac, and T. D. Little, "Adaptive receiver for indoor visible light communications," Journal of Lightwave Technology, vol. 31, no. 23, pp. 3676-3686, 2013.

[15] J. Carruther and J. M. Kahn, "Angle diversity for nondirected wireless infrared communication," Communications, IEEE Transactions on, vol. 48, no. 6, pp. 960-969, 2000.

[16] K. L. Sterckx, J. M. Elmirghani, and R. A. Cryan, "Pyramidal fly-eye detection antenna for optical wireless systems," vol. 5, pp. 1-5, 1999.

[17] A. Hussein, M. Alresheedi, and J. Elmirghani, "20 Gbps Mobile Indoor Visible Light Communication System Employing Beam Steering and Computer Generated Holograms," Journal of Lightwave Technology vol. 33, no. 24, pp. 5242-5260, 2015.

[18] J. R. Barry, J. M. Kahn, W. J. Krause, E. Lee, and D. G. Messerschmitt, "Simulation of multipath impulse response for indoor wireless optical channels," Selected Areas in Communications, IEEE Journal on, vol. 11, no. 3, pp. 367-379, 1993.

[19] M. T. Alresheedi and J. M. Elmirghani, "10 Gb/s indoor optical wireless systems employing beam delay, power, and angle adaptation methods with imaging detection," Journal of Lightwave Technology, vol. 30, no. 12, pp. 1843-1856, 2012.

[20] M. Ingels and M. S. Steyaert, "A 1-Gb/s, 0.7-µm CMOS optical receiver with full rail-to-rail output swing," Solid-State Circuits, IEEE Journal of, vol. 34, no.7, pp. 971-977, 1999.

[21] L. Schmalen, A. J. de Lind van Wijngaarden, and S. t. Brink, "Forward error correction in optical core and optical access networks," Bell Labs Technical Journal, vol. 18, no. 3, pp. 39-66, 2013.